Autoxidation of Pentaammineruthenium(III)-Nucleoside Complexes: Xanthine Oxidase Activity in a Simple Compound without Oxo Atom Transfer

K. C. Gariepy, M. A. Curtin, and M. J. Clarke*

Contribution from the Department of Chemistry, Boston College, Chestnut Hill, Massachusetts 02167. *Received June 30, 1988*

Abstract: The autoxidation of 7-[(Ino)$(NH_3)_5Ru]^{3+}$ and 7-[(1-MeIno)$(NH_3)_5Ru]^{3+}$ proceeds rapidly at high pH to yield the corresponding 8-keto complexes. These reactions have been studied as a function of pH and oxygen concentration and obey the rate law $d[(8\text{-O-Ino})Ru]/dt = k_1k_2[(Ino)Ru][O_2]/(k_{-1}[H^+] + k_2[O_2])$. The reaction with 7-[(Ino)$(NH_3)_5Ru]^{3+}$ exhibits a secondary kinetic isotope effect of $k_H/k_D = 1.6 \pm 0.3$. Running the reaction in $H_2{}^{18}O$ resulted in 80% substitution of ^{18}O in the oxidized product. At 25 °C the specific rates for the Ino and MeIno complexes, respectively, are $k_1k_2/k_{-1} = (7 \pm 2) \times 10^{-11}$ and $(9 \pm 2) \times 10^{-10}$ s^{-1} and $k_1 = (6 \pm 1) \times 10^{-4}$ and $(4 \pm 1) \times 10^{-4}$ s^{-1}. Activation parameters are $\Delta H^* = 54 \pm 4$ kJ/mol and $\Delta S^* = -120 \pm 21$ J/(mol·K) for the Ino complex. The rate law, kinetic isotope effect, and isotopic labeling are consistent with a mechanism involving proton ionization at the C8 position followed by autoxidation as the rate-limiting step.

Platinum group ions exhibit both mutagenic and chemotherapeutic activities in which the initial lesion is thought to be metal ion binding to the N7 of purine residues on DNA.[1,2] Metal ion complexes can also facilitate the hydrolysis[3,4] and oxidative cleavage of nucleic acids in reactions involving the sugar moiety.[5-8] In the presence of ascorbate and hydrogen peroxide, some transition metal ions generate hydroxyl radical, which may attack either the sugar[9] or the C8 position of purines to yield 8-oxopurines on DNA.[10] The molybdenum-containing enzyme xanthine oxidase, whose excess activity is responsible for gout, metabolizes xanthine to uric acid by catalyzing purine oxidation at C8.[11,12] This oxidation can also be effected electrochemically through a single-electron oxidation of xanthosine.[13]

In an earlier study, we showed that coordination of a transition metal to deoxyguanosine facilitated autoxidation of the nucleoside in basic media to yield the corresponding 8-oxoguanosine complex.[14] While side reactions resulting in a dark precipitate precluded a precise, quantitative study of this system, similar reactions occur with other purines and proceed fairly cleanly with hypoxanthine nucleosides.[15] Since this reaction has possible implications for the oncological activity of platinum group metals coordinated to DNA and results in products similar to those generated by xanthine oxidase, we have investigated the process whereby $(NH_3)_5Ru^{III}$ coordinated to the N7 of inosine induces autoxidation of 8-oxoinosine. These ligands are illustrated in Figure 1.

Experimental Section

Synthesis. [Cl$(NH_3)_5Ru]Cl_2$,[16,17] *cis*-[$Cl_2(NH_3)_4Ru]Cl$,[18] and *cis*-[$Cl_2(NH_3)_4Ru](F_3CSO_3)$[19] were prepared by literature syntheses. Inosine (Ino), 2′-deoxyinosine (dIno), xanthosine, and uric acid were purchased from Sigma Chemical Co., St. Louis, MO, and used without further purification. 7-[(Ino)$(NH_3)_5Ru]Cl_2$, 7-[(dIno)$(NH_3)_5Ru]Cl_2$, 7-[(Hyp)$(NH_3)_5Ru]Cl_2$ (Hyp = hypoxanthine), and 7-[(1-MeIno)-$(NH_3)_5Ru]Cl_2$ (1-MeIno = 1-methylinosine) were prepared by previously reported methods.[20] 8-Oxoinosine (8-O-Ino) was prepared in a manner similar to that for 2-amino-9-β-D-ribofuranosyl-6,8-purinedione in which a benzyloxy group is used to introduce a keto function at C8,[21] yield 79%: compound decomposes upon heating with no distinct melting range; HPLC k' 0.21; $\nu_{C=O}$ 1682 (s), 1712 (s); ^1H NMR (DMSO) sugar proton assignments by COSY δ 8.02 (H2), 5.66 (d, H1′), 4.74 (tr, H2′), 4.11 (t, H3′), 3.85 (q, H4′), 3.53 (qd, H5′). Anal. Calcd for $C_{10}H_{12}N_4O_9 \cdot 1.25H_2O$: C, 39.16; H, 4.76; N, 18.26; O, 37.82. Found: C, 39.22; H, 4.10; N, 18.06; O, 37.64.

7-[(8-O-Ino)$(NH_3)_5Ru]Cl_2$ was prepared by direct coordination of 8-O-Ino and by oxidation of coordinated Ino. In the first method, the synthesis is analogous to that of 7-[(Ino)$(NH_3)_5Ru]Cl_2$,[20] except that the pH of the solution of $[H_2O(NH_3)_5Ru^{II}](CF_3CO_2)_2$ was adjusted to about 8 before addition of 8-oxoinosine in 10% excess. The desired product was isolated as a blue band eluted from Bio-Rex 70 with 0.4 M ammonium formate. A second ion-exchange chromatography was done on Dowex 50 eluted with 2 M HCl to exchange the formate anion for chloride. The final product was crystallized from 1 M HCl following rotary evaporation. In the second method, 7-[(Ino)$(NH_3)_5Ru]^{3+}$ was first prepared and purified on a Bio-Rex 70 column eluted with 0.8 M ammonium formate. The pH of this solution was then adjusted to 11.7 with concentrated NH_4OH, yielding a magenta solution. Oxygen or air was slowly bubbled through the solution overnight, and purification was effected as above. An analytically pure sample was obtained by repeating the chromatography on both Bio-Rex and Dowex columns before final precipitation was induced by the addition of absolute ethanol to a minimum volume of the compound in water. HPLC k' 1.54; ^1H NMR (D_2O, pD 1) δ -36.2 (H2) and sugar protons at 7.71, 7.31, 5.56, 5.25, and 4.56; ^1H NMR (D_2O, pD 11.5) -46.0 (H2); ESR $g_\parallel = 2.51$ and $g_\perp = 2.68$ in ethylene glycol/water (1:1) at -77 °C. Anal. Calcd for [(8-*O*-Ino)$(NH_3)_5Ru]$-$Cl_2 \cdot 0.5H_2O$: C, 21.87; H, 4.95; N, 22.95. Found: C, 22.18; H, 5.03; N, 22.28.

7-[(8-O-Hyp)$(NH_3)_5Ru]Cl_2$ (8-O-Hyp = 8-oxohypoxanthine) was prepared in a manner similar to that for 7-[(8-O-Ino)$(NH_3)_5Ru]Cl_2$

(1) Clarke, M. J. *Met. Ions Biol. Syst.* **1980**, *11*, 231-83.
(2) Nicolini, M. *Platinum and Other Metal Coordination Compounds in Cancer Chemotherapy*; Nijhoff Publishing: Boston, MA, 1987.
(3) Schaaper, R. M.; Koplitz, R. M.; Tkshelashvili, L. K.; Loeb, L. A. *Mutat. Res.* **1987**, *177*, 179-88.
(4) Iverson, B.; Dervan, P. B. *J. Am. Chem. Soc.* **1987**, *109*, 1241-3.
(5) Wade, W.; Dervan, P. B. *J. Am. Chem. Soc.* **1987**, *109*, 1574-5.
(6) Stubbe, J.; Kozarich, J. W. *Chem. Rev.* **1987**, *87*, 1107-36.
(7) Richter, H. W.; Rahhal, S. *J. Am. Chem. Soc.* **1988**, *110*, 3126-33.
(8) Clarke, M. J.; Jansen, B.; Marx, K. A.; Kruger, R. *Inorg. Chem. Acta* **1986**, *124*, 13-28.
(9) Youngquist, R. S.; Dervan, P. B. *J. Am. Chem. Soc.* **1985**, *107*, 5528-9.
(10) Kasai, H.; Nishimura, S. *Nucleic Acid. Res.* **1984**, *122*, 2137-45.
(11) Coughlan, M. *Molybdenum and Molybdenum Containing Enzymes*; Pergamon Press: New York, 1980.
(12) *Molybdenum Enzymes*; Spiro, T. G., Ed.; Wiley-Interscience: New York, 1985.
(13) Tyagi, S. K.; Dryhurst, G.J. *Electroanal. Chem.* **1987**, *216*, 137-56.
(14) Clarke, M. J.; Morrissey, P. E. *Inorg. Chim. Acta* **1984**, *80*, L69-70.
(15) Curtin, Maria, unpublished work, 1985.
(16) Vogt, L. H.; Katz, J. L.; Wiberly, S. E. *Inorg. Chem.* **1965**, *4*, 1157.
(17) Allen, A. D.; Bottomley, F.; Harris, R. O.; Reinslau, V. P.; Senoff, C. V. *J. Am. Chem. Soc.* **1967**, *89*, 5595.
(18) Pell, S. D.; Sherban, M. M.; Tramontano, V.; Clarke, M. J. *Inorg. Synth.*, in press.
(19) Diamond, S. E. Ph.D. Thesis, Stanford University, 1975.
(20) Clarke, M. J. *Inorg. Chem.* **1977**, *16*, 738-44.
(21) Holmes, R. E.; Robins, R. K. *J. Am. Chem. Soc.* **1965**, *87*, 1772-6.

0002-7863/89/1511-4947$01.50/0

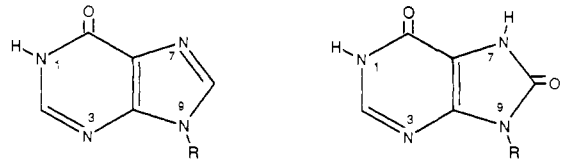

Figure 1. Structures of inosine (Ino), 8-oxoinosine (8-O-Ino), and related hypoxanthine (Hyp) ligands, indicating numbering system.

(method 2) except that the initial ligand was 2'-deoxyinosine and the base was added directly to the bubble flask following oxidation by oxygen. The progress of the oxidation reaction was checked periodically by HPLC. After completion, the bright blue complex was purified by sequential chromatographies on Bio-Rex 70 (eluted with 0.2 M formate) and Dowex 50 (eluted with 2 M HCl) columns. Several small colored bands were observed on Bio-Rex but discarded. After elution from the Dowex column, the blue solution was allowed to stand in the acid for several hours to effect complete hydrolysis of the sugar. After evaporating to dryness, the complex was rechromatographed on the two columns. The residue collected after rotary evaporation was dissolved in water and then precipitated by the addition of ethanol. This solid was dissolved in a minimum amount of water, filtered through a 45-μm Millepore filter, and then reprecipitated by ethanol diffusion: yield 80%; HPLC k' 1.39; ^{1}H NMR (δ) for H2 in D_2O (pD 2.3) −38.3, (pD 8.6) −39.1, (pD 12.03) −50.0. Anal. Calcd for $[(8\text{-O-Hyp})(NH_3)_5Ru]Cl_2$: C, 14.71; H, 4.44; N, 30.88. Found: C, 14.99; H, 4.30; N, 30.65.

8-D-Ino was prepared by dissolving inosine in D_2O and heating for 4 h at 105 °C and collecting crystals on cooling.[22] The yield of the deuterium exchange was determined by NMR with the C2 proton peak height as an internal standard, yield 93%. $7\text{-}[(8\text{-D-Ino})(NH_3)_5Ru]Cl_2$ was prepared by a literature method using 8-D-Ino.[20]

8-^{18}O-Ino was obtained by dissociation from $7\text{-}[(8\text{-}^{18}\text{O-Ino})(NH_3)_5Ru]^{2+}$, which was prepared by dissolving 25 mg of dry $7\text{-}[(\text{Ino})(NH_3)_5Ru]Cl_2$ in 1.0 mL of $H_2{}^{18}O$ (Icon Services, 98 atom % before use, analyzed as 80% by mass spectrometry after recovery by distillation) in a reaction vial. After a small amount of ammonia was allowed to diffuse into the solution until it turned purple-blue, the oxidation reaction proceeded under O_2 until the solution changed to a clear royal blue. After the $H_2{}^{18}O$ was reclaimed by low-pressure distillation, the blue residue was dissolved in water, and the ligand was dissociated by reducing the complex until colorless over Zn(Hg) under argon at pH 2. After a few drops of NH_4OH were added to neutralize the solution, it was loaded onto a Dowex column, and the desired fraction was eluted with water. This was rotary evaporated to dryness, dissolved in water, filtered, and rotary evaporated again.

Compound Characterization. NMR spectra were obtained on a Varian Model XL300 NMR in either D_2O or DMSO with TSP as an internal standard. DCl and NaOD were used to adjust the pD (measured with a pH electrode and corrected by adding 0.4). EPR spectrum were taken of millimolar solutions of $7\text{-}[(\text{Ino})(NH_3)_5Ru]Cl_2$ dissolved in ethanol/water (1:1, CAPS buffer, pH 10.5–12.3), 0.1 M in DMPO (5,5-dimethyl-]-pyrroline *N*-oxide), in 1 mm i.d. tubes saturated with air at 25 °C on a Varian E-9 spectrometer. Infrared spectra were acquired in KBr disks at 0.5% sample concentration on a Perkin–Elmer Model 1430 IR spectrophotometer. UV–visible spectra were obtained on a Perkin Elmer Model 575 spectrophotometer interfaced to an IBM XT microcomputer equipped with a digital plotter. Spectrophotometric pK_a values were determined by regression analysis with the equation $pK_a = pH - \log [(A_b - A_{pH})/(A_{pH} - A_a)]$, where A_b is the absorbance of the deprotonated form of the complex, A_a is that for the acidic form, and A_{pH} is the net absorbance at a given pH. Mass spectral analyses were performed by the NIH regional center at Rockefeller University. A correction for the natural abundance of the P + 2 peak in the ^{18}O-labeled samples was made by standard methods.[23]

The concentration of ruthenium in aqueous samples was determined on an IL 300 atomic absorption spectrophotometer.[24] Oxygen concentrations in aqueous solution were determined with a Model MI-730 micro oxygen probe (Microelectrodes Inc., Londonderry, NH) using a PAR 174A polarographic analyzer (0.02 μA, $E_{appl} = -0.700$ V) equipped with a Houston Instrument 2000 recorder. Standard concentrations were calculated from the appropriate Bunsen coefficients for varying temperatures.[25]

HPLC separations were done on a 300 × 4.6 mm Waters 5-μm, C_{18} column fitted to a Gilson 111B UV detector set at 254 nm with the solvent pumped at 2.00 mL/min by an IBM LC 9521 Isocratic modular pump. The eluent was 0.602 M propionic acid, 10.0 mM sodium hexanesulfonate, and 18.6 mM 1-butanol, adjusted to pH 3.91 with ammonium hydroxide. All solutions were filtered through a 0.45-μm Millepore filter, degassed, and sonicated before use. The system was allowed to equilibrate for 1 h prior to use. Analyte standards around 0.2 mM were injected until the peaks had constant capacity factors and peak heights. The linearity of peak heights versus concentration was verified for each component.

Cyclic voltammetric and square-wave voltammetric experiments were performed on an electrochemical apparatus constructed in this laboratory. All measurements were determined in aqueous buffer at $\mu = 0.1$ adjusted with LiCl. Working electrodes were carbon paste or a platinum disk; a platinum wire served as the counter electrode and Ag/AgCl as the reference electrode. Hexaammineruthenium(III) chloride ($E^\circ = 57$ mV) was used as an internal standard to automatically correct for junction potentials, etc.[26] Data for Pourbaix (potential versus pH) diagrams were obtained by adjusting the pH of the solution in the cell with 0.1 M HCl, 0.1 M LiOH, or appropriate buffer solution and averaging the pH reading before and after the square-wave voltammetric reading, which was internally referenced to the potential of $[(NH_3)_6Ru]^{3+,2+}$. The curve of potential versus pH for $7\text{-}[(8\text{-O-Ino})(NH_3)_5Ru^{III,II}]$ was fitted by standard nonlinear regression methods[27] to

$$E_h = E^f - 0.591 \log \frac{[H^+] + K_1^{III}}{[H^+] + K_1^{II}}$$

where E^f is the formal reduction potential, K_1^{III} is the N1 ionization constant for the ruthenium(III) complex, and K_1^{II} is that for the corresponding ruthenium(II) species. The Pourbaix diagram for $7\text{-}[(8\text{-O-Hyp})(NH_3)_5Ru^{III,II}]$ was fit to

$$E_h = E^f - 0.0591 \log \frac{[H^+]^2 + [H^+]K_9^{III} + K_1^{III}K_9^{III}}{[H^+]^2 + [H^+]K_9^{II} + K_1^{II}K_9^{II}}$$

where E^f, K_1^{III}, and K_1^{II} have the same meanings as above and K_9^{III} and K_9^{II} are the ionization constants for proton loss from N9 of the oxidized and reduced forms, respectively.

Kinetic Measurements. Reactant mixtures often had small amounts of $7\text{-}[(\text{Hyp})(NH_3)_5Ru]Cl_2$ present as a contaminant of the starting material; however, this remained unchanged throughout the course of the reaction. Reactions were run in the following buffers in the ranges indicated: CAPSO [3-(cyclohexylamino)-2-hydroxy-1-propanesulfonic acid, pH 8.9–10.3]; CAPS [3-(cyclohexylamino)-1-propanesulfonic acid, pH 9.7–11.1], and Na_2HPO_4/Na_3PO_4 (pH 11.32–13.02). Buffer concentrations were 0.01 M with the ionic strength adjusted to 0.1 with LiCl. The pH of the solution was redetermined at each temperature with a pH electrode calibrated with standard buffers at the same temperature. The temperature was monitored by a Fluke Instruments 52 K/J or YSI 32 meter with a thermistor probe. Oxygen concentrations were determined prior to each run and monitored to verify that a constant concentration was maintained throughout the reaction. Oxygen concentrations were varied with customized O_2/N_2 gas mixtures (Linde) of 50% and 75% in addition to air and pure O_2. The temperature was constant to within ±0.15 °C, and the pH of the solution generally did not vary greater than ±0.03 unit during the course of each study. The deuterium isotope effect was determined by running reactions with $7\text{-}[(\text{Ino})(NH_3)_5Ru]Cl_2$ and $7\text{-}[(8\text{-D-Ino})(NH_3)_5Ru]Cl_2$ simultaneously in the same aqueous buffer and temperature bath at 25 °C, pH 10.17 and pO_2 0.209.

In order to determine whether H_2O_2 formed subsequent to the autoxidation process also oxidized $7\text{-}[(\text{Ino})(NH_3)_5Ru^{III}]$, the rate was determined in the presence of catalase (Sigma, 2800 units/mg). The activity of the catalase under the basic reaction conditions (0.1 M LiCl/0.1 M CAPS buffer, pH 10.2, 60 units/mL of catalase) was verified by measuring the rate of disappearance of H_2O_2 by observing the decrease in absorbance at 240 nm and comparing it to that of the same reaction at pH 7. The rate of autoxidation of the complex was determined under

(22) Schweizer, M. P.; Chan, S. I.; Helmkamp, G. K.; Ts'o, P. O. P. *J. Am. Chem. Soc.* **1964**, *86*, 696–700.

(23) Biemann, K. *Mass Spectrometry, Organic Chemical Applications*; McGraw-Hill: New York, 1962; pp 60–9.

(24) Clarke, M. J. *J. Am. Chem. Soc.* **1978**, *100*, 5068–75.

(25) Battino, R.; Clever, H. L. *Chem. Rev.* **1966**, *66*, 398.

(26) Lim, H. S.; Barclay, D. J.; Anson, F. C. *Inorg. Chem.* **1972**, *11*, 1460. Yee, E. L.; Cave, R. J.; Guyer, K. L.; Tyma, P. D.; Weaver, M. J. *J. Am. Chem. Soc.* **1979**, *101*, 1131. Matsubara, T.; Ford, P. C. *Inorg. Chem.* **1976**, *15*, 1107.

(27) SAS Institute Inc., Cary, NC 27511. Nonlin procedure using the Dudley algorithm and unit weighting.

Table I. UV–Visible Spectra of 7-[$L(NH_3)_5Ru^{III}$][a]

ligand	deprotonation site	λ (nm)	ε (10^3 M^{-1} cm^{-1})
Ino[b]		249	10.1
		305	1.08
		455	0.27
Ino^-	1	260	10.0
		300 sh	1.20
		351 sh	0.59
		524	0.33
8-O-Ino^-	7	265	10.59
		298 sh	5.45
		379	1.60
		605	2.23
8-O-Ino^{2-}	1, 7	268	11.2
		304 sh	2.35
		346 sh	1.58
		648	2.29
Hyp[b]		247	10.3
		300	1.33
		461	0.316
Hyp^-	9	237 sh	7.59
		255	9.69
		357	2.02
		529	0.859
Hyp^{2-}	1, 9	261	9.7
		312	2.00
		402	1.14
		588	11.7
8-O-Hyp^-	7	265	12.8
		292 sh	5.32
		371	1.19
		609	1.90
8-O-Hyp^{2-}	1, 7	266	13.1
		359	1.34
		653	1.95
8-O-Hyp^{3-}	1, 7, 9	273	28.7
		315 sh	2.98
		354 sh	1.77
		412 sh	1.37
		741	2.17

[a] μ = 0.1 adjusted with LiCl. Spectra of deprotonated ligand species taken at least 2 pH units above the pK_a. sh = shoulder. [b] Clarke, M. J. *Inorg. Chem.* **1977**, *16*, 738–44.

the same conditions and compared to a control lacking catalase. The possible role of superoxide was similarly assessed with superoxide dismutase (Sigma, 3000 units/mg) under identical reaction conditions.

To determine whether H_2O_2 oxidized the complex, 1.5 mL of 0.524 mM H_2O_2 (21 μL of 30% H_2O_2 diluted to 500 mL) was added to 1.5 mL of 0.2 M LiCl/0.02 M CAPS buffer at pH 10.27. After argon was bubbled through the solution to remove oxygen, solid 7-[(Ino)-$(NH_3)_5Ru]Cl_2$ was introduced to give a concentration of 0.1 mM, and the rates were determined as stated above.

Results

Compound Characterization. The ^1H NMR spectra of 7-[(8-O-Ino)$(NH_3)_5Ru^{III}]^{2+}$ at pD 0.9 revealed that the peak attributed to the C8 proton in the corresponding spectrum of 7-[(Ino)-$(NH_3)_5Ru]^{3+}$ at −15.7 ppm had vanished. This peak was also not evident in the ^1H NMR spectrum of 7-[(8-O-Hyp)$(NH_3)_5Ru]Cl_2$. The resonance attributed to H2 of 7-[(8-O-Ino)$(NH_3)_5Ru^{III}]^{2+}$ shifted from 8.02 in the free ligand to −37 ppm, and the sugar protons, which are clustered between 3.5 and 5.5 ppm in the free ligand and exhibit clear coupling to adjacent protons, appeared as relatively broad lines between 4.5 and 7.7 ppm with no apparent coupling. The resonances of the sugar protons were not assigned, since no coupling pattern could be observed even by 2D COSY.[28] The infrared, ^1H NMR, and mass spectra of 8-O-Ino obtained from dissociation from the ruthenium complex and an authentic, synthetic sample were identical. Similarly, electronic spectra (see Table I) obtained from the oxidized product of 7-[(Ino)-$(NH_3)_5Ru]^{3+}$ and 7-[(8-O-Ino)$(NH_3)_5Ru^{III}]^{2+}$ prepared from the reaction of $[(H_2O)(NH_3)_5Ru]^{2+}$ and 8-O-Ino were identical. The

(28) Bailey, V.; Clarke, M. J., unpublished data, 1988.

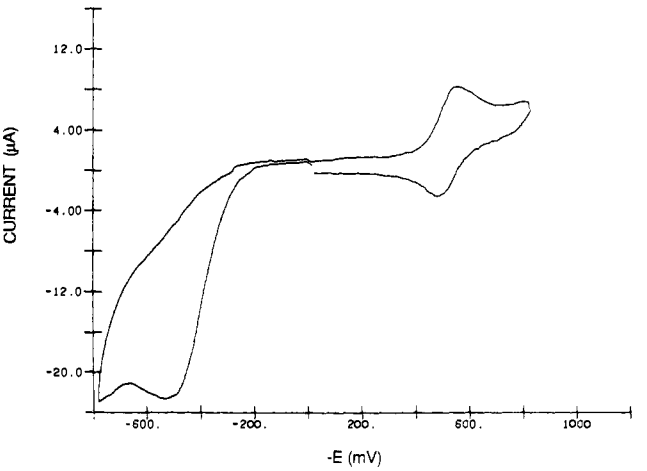

Figure 2. Second cyclic voltammetry scan of 7-[(8-O-Ino)$(NH_3)_5Ru^{III}]^{2+}$ in 0.09 M LiCl–0.01 M phosphate buffer at pH 12.2 showing irreversible oxidation process.

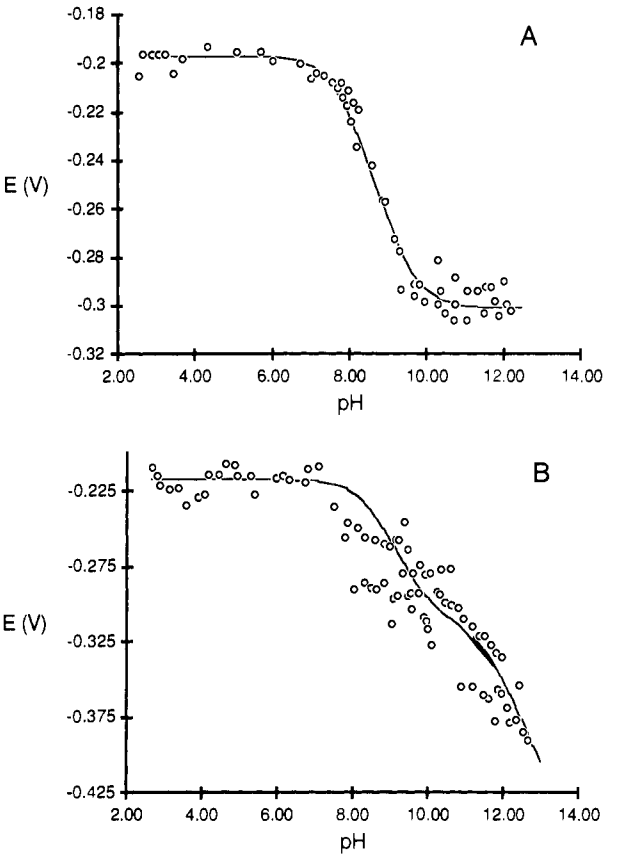

Figure 3. (A) Plot of reduction potential versus pH (Pourbaix diagram) for 7-[(8-O-Ino)$(NH_3)_5Ru^{III,II}]$. (B) Pourbaix diagram of 7-[(8-O-Hyp)$(NH_3)_5Ru^{III,II}]$.

H2 ^1H NMR signal of 7-[(8-O-Hyp)$(NH_3)_5Ru^{III}]$ varied substantially on deprotonation from −38.3 ppm at pD 2.43 to −50 ppm at pH 12.

While electrochemical properties of 7-[(Ino)$(NH_3)_5Ru]Cl_2$ have been previously published,[20] the purine oxidation reported here prompted another look at the anodic processes. Despite the fact that autoxidation occurs rapidly above pH 9.5, no evidence of a ligand oxidation current could be detected with carefully purified samples under anaerobic, basic conditions up to the limits of the electrode and solvent.

A typical cyclic voltammetry scan of 7-[(8-O-Ino)-$(NH_3)_5Ru^{III}]^{2+}$ is shown in Figure 2. On initial scans, only the reversible wave at −198 mV (vs NHE), attributed to the Ru(III,II) couple, was observed. On subsequent scans, the irreversible ox-

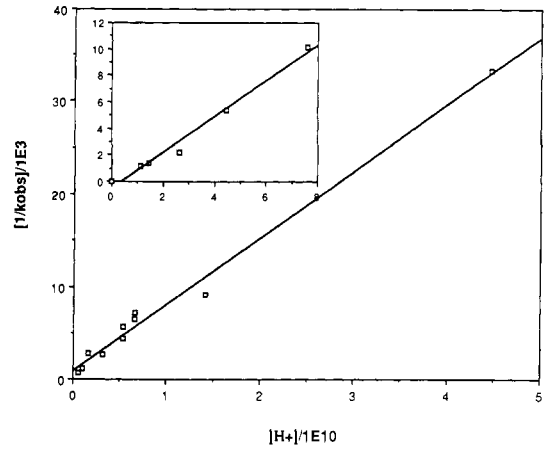

Figure 4. Plot of $1/k_{obs}$ versus $[H^+]$ for 7-[(Ino)$(NH_3)_5$Ru]Cl_2. (Inset) Plot of $1/k_{obs}$ versus $[H^+]$ versus $[H^+]$ for 7-[(1-MeIno)$(NH_3)_5$Ru]Cl_2.

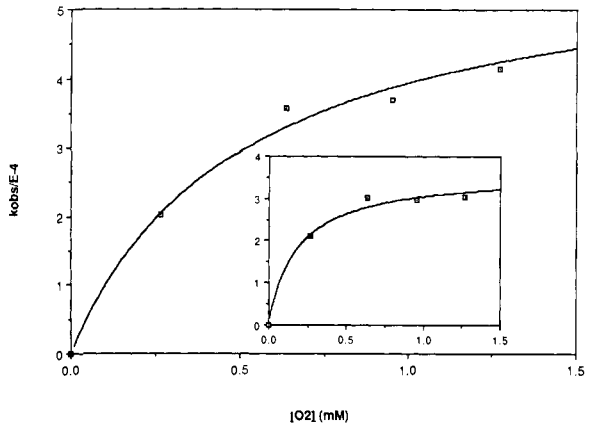

Figure 5. Plot of k_{obs} versus $[O_2]$ for 7-[(Ino)$(NH_3)_5$Ru]Cl_2. (Inset) Plot of k_{obs} versus $[O_2]$ for 7-[(1-MeIno)$(NH_3)_5$Ru]Cl_2.

idation wave at about 520 mV (vs NHE) became apparent. This wave may be due to oxidation of the ligand following dissociation from the reduced complex. A Pourbaix diagram for this complex as determined by square-wave voltammetry is shown in Figure 3A and indicates $E°$ = −198 ± 5 mV (vs NHE) and pK_a values of 7.76 ± 0.06 and 9.52 ± 0.06 for ionization of the N1 proton of the Ru(III) and Ru(II) complexes, respectively. Spectrophotometric titration of 7-[(8-O-Hyp)$(NH_3)_5Ru^{III}]^{2+}$ yielded pK_a values of 8.36 ± 0.01 and 11.41 ± 0.02 for the N9 and N1 protons, respectively. The Pourbaix diagram for this complex shown in Figure 3B shows the Ru(III,II) reduction potential to be −218 ± 10 mV with pK_a = 9.9 ± 0.1 for ionization of the N9 proton from the Ru(II) complex, when the pK_a values for the Ru(III) complexes are constrained to be those spectrophotometrically determined in the least-squares fit. Loss of the N1 proton occurs at a pK_a greater than 12 for the Ru(II) species.

Kinetics. As indicated in Figure 4, the oxidations of both 7-[(Ino)$(NH_3)_5$Ru]$^{3+}$ and 7-[(1-MeIno)$(NH_3)_5$Ru]$^{3+}$ were found to be inversely dependent on acid concentration. At similar pH and oxygen concentrations, the oxidation of the 1-MeIno complex proceeded 3–10 times more rapidly than that of the inosine complex. The effect of oxygen concentration on the rate was more complicated and exhibited a saturation effect as seen in Figure 5. The empirical rate law derived from these data is $(\text{rate})^{-1} = \{[H^+]/k_a[O_2] + 1/k_b\}[(\text{Ino})\text{Ru}]^{-1}$, where k_a and k_b can be derived from plots of $(k_{obs})^{-1}$ versus either $[H^+]$ or $1/[O_2]$. Values of k_a and k_b derived from either type of plot agreed within experimental error and are for the oxidation of 7-[(Ino)$(NH_3)_5$Ru]$^{3+}$ and 7-[(1-MeIno)$(NH_3)_5$Ru]$^{3+}$, respectively: $k_a = (7 \pm 2) \times 10^{-11}$ s^{-1} and $(9 \pm 2) \times 10^{-10}$ s^{-1} and $k_b = (6 \pm 1) \times 10^{-4}$ s^{-1} and $(4 \pm 1) \times 10^{-4}$ s^{-1}. An Eyring plot of the observed rate constants normalized for variations in oxygen concentration (P_{O_2} = 0.209) at pH 10.27 is shown in Figure 6 for the inosine complex. Activation

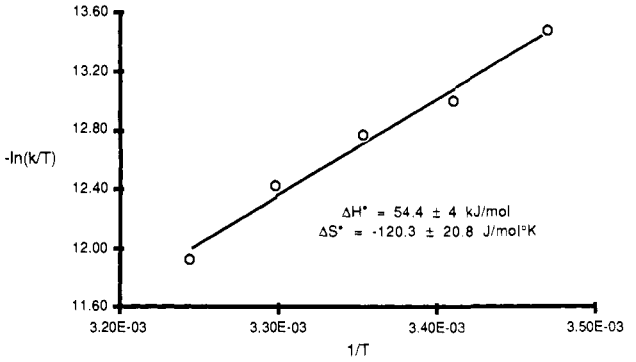

Figure 6. Eyring plot of k'_{obs} versus $[1/T]$ for 7-[(Ino)$(NH_3)_5$Ru]Cl_2. Observed rate constants are normalized for varying oxygen concentrations at the various temperatures.

parameters are ΔH^* = 54 ± 4 kJ/mol and ΔS^* = −120 ± 21 J/(mol·K).

Running the reaction in the presence of radical scavengers, DMPO,[29] and 50% ethanol at room temperature resulted in no immediately observable radicals by ESR at pH 10.5. However, after 45 min under these conditions, a weak signal was obtained. At pH 11.5 a signal was evident after 15 min, and a strong signal was obtained after 45 min. At pH 12.3, a good signal was present as soon as the sample was placed in the instrument. The signal obtained, while reproducible and reminiscent of hydroxylated DMPO•, showed evidence of DMPO decomposition,[29] with splitting evident in the DMPO signal and a triplet growing in at longer reaction times between the DMPO resonances. A close simulation of the initial spectra could be obtained by assuming coupling due the three spin systems with values of $a_1 = 19.84 \times 10^{-4}$ cm^{-1} (I = 1), $a_2 = 15.2 \times 10^{-4}$ cm^{-1} ($I = {}^1/_2$), and $a_3 = 2.2 \times 10^{-4}$ cm^{-1} (I = 1), which are consistent with coupling to a ^{14}N, a ^{1}H, and a second ^{14}N, respectively. The second signal arising at longer times showed a 1:2:1 triplet pattern with a = 19.2 G.

Observed rate constants for the autoxidation of 7-[(Ino)-$(NH_3)_5Ru^{III}$] at pH 10.2 in the presence of either catalase or superoxide dismutase were identical with control experiments, indicating that neither superoxide nor peroxide participates significantly in the autoxidation process. Oxidation of 7-[(Ino)-$(NH_3)_5Ru^{III}$] in 0.27 mM solutions of H_2O_2 (no catalase added) occurred rapidly with oxygen effervescence, indicating that the ruthenium compound catalyzes the disproportion of H_2O_2. In this reaction, oxidation by O_2 and/or H_2O_2 may be occurring, since the P_{O_2} during these reactions was unity, owing to the effervescence following peroxide disproportionation, and the k_{obs} (5.9×10^{-4} s^{-1}) is in the range expected for P_{O_2} = 1. In the autoxidation reactions, the concentration of H_2O_2 would always remain substantially below that of O_2, and oxidation by H_2O_2 generated by autoxidation would not be significant, consistent with the catalase experiments. Running the reaction in the presence of a radical scavenger (50% ethanol) at 23 °C and pH 10.75 in air gave a 24% decrease in the observed rate constant, $(2.7 \pm 0.2) \times 10^4$ s^{-1}, versus that in aqueous solution under the same conditions, $(3.7 \pm 0.4) \times 10^4$ s^{-1}.

The observed rate constants for the oxidation of 7-[(Ino)-$(NH_3)_5Ru^{III}$] and 7-[(8-D-Ino)$(NH_3)_5Ru^{III}$] at 25 °C and pH 10.2 under atmospheric oxygen were $(1.5 \pm 0.1) \times 10^{-4}$ s^{-1} and $(0.92 \pm 0.08) \times 10^{-4}$ s^{-1}, respectively, yielding a deuterium isotope effect (k_h/k_d) of 1.6 ± 0.3. Mass spectral analysis of 8-O-Ino formed on oxidizing 7-[(Ino)$(NH_3)_5$Ru]Cl_2 in $H_2{}^{18}O$ yielded an 80% relative abundance of the ^{18}O-labeled product, which was identical with the fraction of ^{18}O in the water recovered from the reaction mixture.

Discussion

Compound Characterization. The peaks centered around 390 and 600 nm in the electronic spectra of the ruthenium(III) com-

(29) Johnson, C. R.; Myser, T. K.; Shepherd, R. E. *Inorg. Chem.* **1988**, *27*, 1089–95.

plexes with 8-O-Ino$^-$ and 8-O-Hyp$^-$ shift toward lower energy on deprotonation of the ligands (cf. Table I) and are attributed to ligand-to-metal ($\pi \rightarrow d_\pi$) charge-transfer transitions. (Superscript charges on ligands are used to indicate deprotonated ligands, and deprotonation sites are indicated in the tables or in the text where these ionized species are discussed.) These bands occur at significantly lower energies relative to the LMCT transitions in the analogous complexes with Ino and Hyp, since the oxidized ligand complexes involve an anionic, rather than neutral, ligand. Perhaps owing to charge location directly at the metal coordination site, the LMCT's in the oxidized ligand complexes are at an even lower energy than the corresponding Ino$^-$ and Hyp$^-$ species, which are deprotonated at sites distant from the coordination position. In concert with the metal ions accepting more of the anionic charge from the ligand, the reduction potentials for $[L(NH_3)_5Ru^{III,II}]$ are about 200–350 mV more negative when L = 8-O-Ino$^-$ or 8-O-Hyp$^-$ than when L = Ino$^-$ or Hyp$^-$.[20] Similarly, the large shifts exhibited by the *H*2 protons in the ^{1}H NMR spectra of 7-$[(8\text{-O-Ino})(NH_3)_5Ru^{III}]$ and 7-$[(8\text{-O-Hyp})(NH_3)_5Ru^{III}]$ suggest the transfer of substantial spin-density onto the ligand, again consistent with the d_π orbital on the metal strongly interacting with the π system of the ligand. The particularly large shifts in the H2 resonance and LMCT bands on removing the last proton from 8-O-Hyp indicate that residual charge on the ligand interacts quite strongly with the metal ion. This suggests that the final proton is removed from the imidazole rather than the pyrimidine ring, i.e., N9 rather than N1. While the ^{1}H NMR resonances of the sugar protons could not be assigned, free 8-O-Ino is known to adopt a syn conformation as a result of steric hindrance at the C8 position,[30] so that the ribose in 7-$[(8\text{-O-Ino})(NH_3)_5]Ru^{III}$] probably also assumes this configuration.

Kinetics and Mechanism. While a large number of N7-coordinated nucleoside complexes are known with a variety of metal centers,[31] metal ion induced oxidation of purine nucleosides to yield 8-oxo nucleosides has not been reported for any other metal ion outside of an enzymic active site, suggesting that the electronic structure of Ru(III) is important in facilitating this reaction. Since the oxidation of the purine is essentially quantitative and not dependent on an external reductant, the generation of a diffusible hydroxyl radical cannot be invoked in any mechanism for this process.[10] Hydroxyl radical requires a three-electron reduction of dioxygen and is unlikely to occur in the absence of an additional reductant.

The half-empty d_π orbital in ruthenium(III) ammine complexes is known to overlap well with π-donor nitrogen ligands such as R–NH$^-$ and imidazolates, which causes the corresponding conjugate acids to be more ionizable than when coordinated to other tripositive metal ions.[24,32] Studies on deprotonation from nitrogen sites in pentaammineruthenium(III) complexes of purines and pyrimidines show that the increase in pK_a is dependent on the inverse square of the distance between the metal ion and the ionizable site.[33] Moreover, imidazolium, metal complexes of imidazole,[34] and protonated purine cations are all known to exchange protons of the carbon between the two imidazole nitrogens. Consequently, it is reasonable to assume that deprotonation from C8 occurs to some extent at high pH and that this is faciliated not only by the proximity of the metal ion but also by transfer of electron density to the partially populated Ru(III) d_π orbital.

Deprotonation to form an anionic purine ligand would significantly lower the oxidation potential for the nucleoside, which for free inosine can be estimated to be around 0.7 V[35] at pH 10. While this potential is within the range of that for the reduction of oxygen to water at the same pH, it is well above that for the two-electron reduction of oxygen to peroxide and substantially above that for the one-electron process forming superoxide. Oxidation of a transiently deprotonated intermediate in low concentration also explains why the ligand oxidation process is not observed electrochemically at pH's where the autoxidation proceeds rapidly.

Scheme I. Proposed Reaction Mechanism for the Autoxidation of 7-$[(Ino)(NH_3)_5Ru]^{3+}$

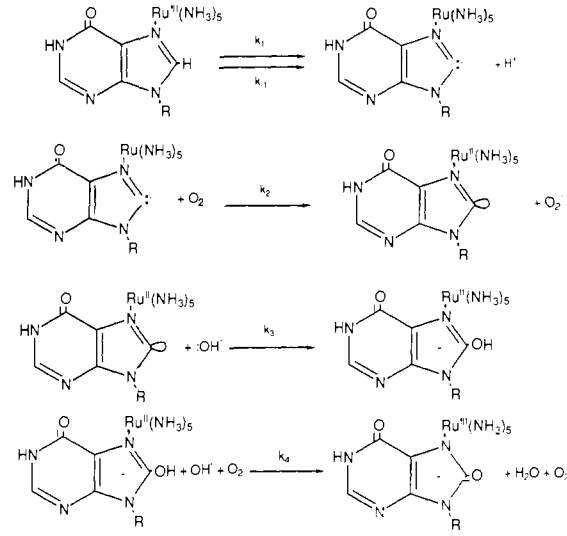

Since the purine oxidation involves two electrons, the formation of either peroxide or superoxide is expected, and lowering of the purine oxidation potential by deprotonation at C8 should make purine oxidation thermodynamically possible for a net two-electron process. However, since no change in the rate was observed in the presence of superoxide dismutase and since the relatively small, 24% decrease in the rate that occurred with 50% ethanol as a radical scavenger may well be due to solvent effects, it is not likely that an O_2^- species participates significantly in the oxidation reaction.

Similarly, since addition of catalase did not significantly affect the reaction, peroxide is not involved in the autoxidation process. Peroxide solutions initially free of O_2 oxidized the complex at nearly the same rate as oxygen-saturated solutions, since the ruthenium complex catalyzes the disproportionation of peroxide. Consequently, any oxidation by peroxide cannot be faster than that by O_2. In harmony with this, the rate of oxidation of $[(NH_3)_6Ru]^{2+}$ by O_2 is almost 6 times than that of H_2O_2.[36,37] In autoxidation reactant solutions, the maximum concentration of H_2O_2 would equal the complex concentration, and this only at the end of the reaction, so that H_2O_2 participates minimally, and probably not at all, in the autoxidation process.

In view of the fact that this reaction only appears on coordination of Ru(III), it may be it proceeds in one-electron steps. Indeed, the introduction of a DMPO as a spin trap resulted in a strong ESR signal as the reaction proceeded through one half-life at high pH. Moreover, the electrochemical oxidation of closely related nucleosides proceeds by a $1e^-$, $1H^+$ process to generate a radical at C8 that can be attacked by water to yield the 8-hydroxylated free radical, which, in turn, undergoes a second $1e^-$, $1H^+$ oxidation to give the 8-keto nucleoside.[38,39]

Transfer of π-electron density from the C8-deprotonated nucleoside to Ru(III) in the manner indicated above would lower its charge so that the canonical form, Ru(II)–Ino$^\bullet$, could reasonably be drawn. Since ammineruthenium(II) complexes undergo facile autoxidation to yield superoxide,[36,40] this portion of

(30) Uesugi, S.; Ikehara, M. *J. Am. Chem. Soc.* **1977**, *99*, 3250–3.
(31) Spiro, T. G. *Nucleic Acid Metal Ion Interactions*; Wiley: New York, 1980.
(32) Hoq, M. F.; Shepherd, R. E. *Inorg. Chem.* **1984**, *23*, 1851–8.
(33) Kastner, M. E.; Coffey, K. F.; Clarke, M. J.; Edmonds, S. E.; Eriks, K. *J. Am. Chem. Soc.* **1981**, *103*, 5747–52.
(34) Rowan, N.; Storm, C.; Rowan, R. *J. Inorg. Biochem.* **1981**, *14*, 59–65.
(35) Dryhurst, G. *Electrochemistry of Biological Molecules*; Academic Press: New York, 1977; p 131.
(36) Stanbury, D. M.; Haas, O.; Taube, H. *Inorg. Chem.* **1980**, *19*, 518–24.
(37) Kristine, F. J.; Johnson, C. R.; O'Donnell, S.; Shepherd, R. E. *Inorg. Chem.* **1980**, *19*, 2280–4.
(38) Subramanian, P.; Dryhurst, G. *J. Electroanal. Chem. Interfacial Electroanal. Chem. Interfacial Electrochem.* **1987**, *224*, 137–62.
(39) Tyagi, S. K.; Dryhurst, G. *J. Electroanal. Chem.* **1987**, *216*, 137–56.

the complex may well be the site of oxygen attack. Assuming a single-electron oxidation, an unstable radical would be formed, which could then undergo hydroxide attack followed by a rapid second electron oxidation. A process with the latter two steps reversed is also conceivable. Induced electron transfer to Ru(III) following a one-electron oxidation of a coordinated ligand is known[41,42] and would lower the activation energy for the first oxidation step by forming a ruthenium(II) complex with the two electron oxidized purine.

Scheme I presents a likely mechanism based on these concepts. The incorporation of ^{18}O into the final product unambiguously indicates that the source of the ketonic oxygen atom is from the solvent and not from molcular oxygen. The small deuterium isotope effect ($k_H/k_D = 1.6$) observed is consistent with the first step in the process being proton dissociation.[43]

An often proposed catalytic mechanism for xanthine oxidase involves molybdenum coordination of the purine at N9 followed by hydride transfer (or its equivalent) from the substrate in concert with an oxo coordinated to the Mo being transfered to the substrate.[44,45] The hydride transfer is suggested to occur to a coordinated sulfide, yielding a Mo(IV) sulfhydryl center.[46] The Mo(IV) passes both electrons in one-electron steps to either (or both) an iron–sulfur moiety or a flavin, which joins the electrons back together in reducing molecular oxygen to peroxide.[47] In the final step, the molybdenum site releases the oxidized purine in a hydrolytic process producing the original oxo, sulfido molybdenum(VI) center. However, other proposed mechanisms are similar to that given in Scheme I.[46]

While in the present system no attempt was made to model the molybdenum center in xanthine oxidase/dehydrogenase and related enzymes and an obvious caveat must be taken in any comparison of the chemistry of Ru(II,III) with that of Mo(IV–VI), it is clear that the oxidation process can be facile in the absence of steric prepositioning by the protein to effect a concerted oxo attack and hydride transfer. Indeed, in the present case, retention of the ammines indicates there is no oxo–metal ion complex formed. While hydroxide attack at C8 in the initial step followed by (or in concert with) hydride transfer[48] to the Ru and subsequent oxidation would also be consistent with the rate law, it would be inconsistent with the small deuterium isotope effect, and no precedent exists for a 7-coordinate, ammineruthenium(III)–hydride complex. Consequently, it appears that the important elements for inducing oxidase activity are coordination by a metal ion with a one or two π-electron sink capable of passing the electrons on to eventually reduce O_2. It is possible that a Mo(VI) center conjugated to a pterin coenzyme could effect purine oxidation in this fashion. While the action of xanthine oxidase must involve the transfer of an oxygen atom from the Mo to some substrates, it is not necessary to invoke a concerted, two-electron process to postulate a reasonable mechanism for purine oxidation, since both the ruthenium-facilitated and the electrochemical[13,49] oxidations of purines proceed by water or hydroxide attack at C8 in an oxidized form rather than oxo atom transfer.

It is likely that the d^5 electronic configuration of Ru(III) is important in facilitating autoxidation and that this reaction is not noteworthy with d^8 ions, such as Pt(II), which also bind to nucleic acids. While, in the present study dealing with a ribo- rather than a deoxyribonucleoside, hydrolytic cleavage of the sugar–purine bond was not important, as suggested by our preliminary study,[14] 8-oxo deoxynucleoside complexes may be inclined toward hydrolysis of the sugar–purine bond. Consequently, metal ion induced oxidation of purines on DNA may weaken the sugar–phosphate backbone of a nucleic acid and eventually result in strand cleavage. Further investigations will center on this problem.

Acknowledgment. This work was supported by PHS Grant GM26390. We are grateful to Prof. Dennis Sardella (BC) for assistance in understanding the deuterium isotope effect and to Prof. Robert C. Bray, University of Sussex, for helpful correspondence. ESR spectra were performed by Maria McNamara and Prof. Hans Van Willigen (University of Massachusetts, Boston). We are in debt to Prof. Rex E. Shepherd (University of Pittsburgh) for helpful discussions.

Supplementary Material Available: Data for all graphs and typical HPLC of reaction (6 pages). Ordering information is given on any current masthead page.

(40) Johnson, C. R.; Myser, T. K.; Shepherd, R. E. *Inorg. Chem.* **1988**, *27*, 1089–1095.
(41) Pell, S. J.; Salmonsen, R.; Abelliera, A.; Clarke, M. J. *Inorg. Chem.* **1984**, *23*, 385–7.
(42) Bryan, D. M.; Pell, S. D.; Kumar, R.; Clarke, M. J.; Rodriguez, V.; Sherban, M.; Charkoudian, J. *J. Am. Chem. Soc.* **1988**, *110*, 1498–1506.
(43) Carpenter, B. *Determination of Organic Reaction Mechanisms*; Wiley: New York, 1984; p 110.
(44) Hille, R.; Sprecher, H. *J. Biol. Chem.* **1987**, *262*, 10914.
(45) Bray, R. C.; George, G. N. *Biochem. Soc. Trans.* **1985**, *13*, 560–7.
(46) Holm, R. H. *Chem. Rev.* **1987**, *87*, 1401–1449.
(47) Skibo, E. B.; Gilchrist, J. H.; Lee, C.-H. *Biochemistry* **1987**, *26*, 3032–7.
(48) Bernhard, P.; Sargeson, A. M.; Anson, F. C. *Inorg. Chem.* **1988**, *27*, 2754–60.
(49) McKenna, K.; Brajter-Toth, A. *J. Electroanal. Chem.* **1987**, *233*, 49–62.